[CANCER RESEARCH 63, 2855–2863, June 1, 2003]

Inhibition of *BUB1* Results in Genomic Instability and Anchorage-independent Growth of Normal Human Fibroblasts[1]

Antonio Musio,[2] Cristina Montagna, Desirée Zambroni, Esterina Indino, Ottavia Barbieri, Lorenzo Citti, Anna Villa, Thomas Ried, and Paolo Vezzoni

Istituto di Tecnologie Biomediche, Consiglio Nazionale delle Ricerche, Via Fratelli Cervi, 93, 20090 Segrate, Milan, Italy [A. M., D. Z., A. V., P. V.]; Genetics Branch, Center for Cancer Research, National Cancer Institute/NIH, Bethesda, Maryland 20892-0913 [C. M., T. R.]; Centro Ricerche Parco Scientifico "E. Menni," Ospedale Poliambulanza, 25100 Brescia, Italy [D. Z.]; Istituto Zooprofilattico Sperimentale delle Regioni Lazio e Toscana, Dipartimento di Firenze, 50010 Florence, Italy [E. I.]; Dipartimento di Oncologia Biologia e Genetica, Università di Genova, I.S.T., 16132 Genoa, Italy [O. B.]; and Istituto di Fisiologia Clinica, Consiglio Nazionale delle Ricerche, 56124 Pisa, Italy [L. C.]

ABSTRACT

The relative contribution of aneuploidy and gene mutations to human tumorigenesis is not yet known. Studies in mice have demonstrated that even single point mutations in oncogenes and tumor suppressor genes can dramatically increase tumor frequency. However, models to evaluate the definitive role of aneuploidy and genomic instability are not yet available. Human fibroblast cells have long been used as a tool for investigating proliferation, senescence, immortalization, and tumorigenesis, all processes that are strongly interrelated. We have now used antisense and ribozyme-mediated temporary inhibition of *BUB1* to study the consequences of mitotic checkpoint failure on the development of aneuploidy. The analysis of cell colonies selected by soft agar growth showed evidence of chromosome instability and delayed senescence, without being tumorigenic in nude mice. Our data suggest that chromosomal instability and aneuploidy are early changes that precede tumorigenicity in the multistep process leading to neoplastic transformation.

INTRODUCTION

Although the notion that aneuploidy is a hallmark of human cancer dates back to the beginning of the last century (1), the exact role that it plays in the pathogenesis of cancer is debated and still essentially unknown (2, 3). In particular, it is not clear whether aneuploidy is merely a consequence of mutations in tumor-causing genes or an intrinsic feature of cancer cells that by itself promotes mutations in these genes (4, 5). Cancer is thought to be a multistep process in which abnormalities in oncogenes and tumor suppressors predispose cells to the acquisition of many other genetic and "epigenetic" changes, which are responsible for the acquisition of the full malignant phenotype, including the ability to invade surrounding tissues and metastatize to distant organs (6). However, there is ample experimental evidence that variation in nuclear DNA content and chromosomal aneuploidies may occur at early stages of tumorigenesis and are invariably observed in carcinomas (2, 7–10). On the basis of these observations, Duesberg *et al.* (11, 12) have recently emphasized the "aneuploidy first" hypothesis.

According to this view, by gaining or losing entire chromosomes, aneuploidy could simulate both overexpression and loss of specific loci relevant to cell growth, thus providing the substrate for selection of more aggressively growing cells (11, 13). Therefore, a role for selection in pathogenesis of cancer (14) is not restricted to the mutation first hypothesis but is shared by the aneuploidy first one.

Recently, the molecular and genetic investigation of human colon cancer led to recognize two different forms of genetic instability: (*a*) the elevated frequency of loss or gain of one or a few whole chromosomes or large parts thereof within the cells of an individual clone (CIN[3]); and (*b*) MIN (15–17).

The genetic basis of MIN has been identified (18), whereas the search for genes responsible for CIN has been essentially negative (3). This raises the possibility that germ-line abnormalities are not responsible for CIN; on the contrary, it could be the exposure to damaging agents, resulting in checkpoint activation, growth arrest, and damage repair, that cause a few cells to abnormally segregate their chromosomes, yet escape apoptosis. These compounds could interfere with molecular complexes involved in spindle checkpoint, resulting in aneuploid cells, some of which could acquire a growth advantage. In this case, aneuploidy would be the first detectable change on which subsequent genomic anomalies would take place.

Human fibroblasts have been used to investigate mechanisms of tumorigenicity. They have a limited proliferative potential, and a combination of two oncogenes and *hTERT* activity is needed for immortalization (4, 5), although data challenge this view (19). In the present study, we set up an *in vitro* model to test the hypothesis that aneuploidy could occur early in transformation in humans. We therefore explored antisense-mediated selective and temporary gene inactivation, *i.e.*, inhibition of gene function without gene mutation. Therefore, this technique would circumvent the use of genotoxic drugs, which act in complex and uncontrolled ways in tumorigenesis. We exposed human fibroblast to antisense oligonucleotides directed against 13 different genes involved in chromosome segregation. We demonstrated that inhibition of several of these genes gives rise to aneuploid cells, most of which are eliminated by apoptosis. After inhibition of *BUB1*, whose product is involved in the spindle checkpoint, some of these cells are able to escape programmed death and give rise, at low frequency, to AI clones. Analysis of these clones shows chromosomal instability and suggests that even temporary interfering with spindle checkpoint genes could be relevant to neoplastic transformation in humans.

MATERIALS AND METHODS

Cell Culture. All of the reported experiments were performed with primary human fibroblast cell line (subject 1), established by skin biopsy from a 4-year-old Caucasian child undergoing surgical procedure (obtained from Niguarda Hospital Tissue Bank, Milan, Italy), and grown in DMEM (Life Technologies, Inc.) supplemented with 10% FCS and antibiotics in a humidified 5% CO_2 atmosphere. Plating efficiency was ~60%. The population

Received 1/17/03; accepted 3/27/03.

The costs of publication of this article were defrayed in part by the payment of page charges. This article must therefore be hereby marked *advertisement* in accordance with 18 U.S.C. Section 1734 solely to indicate this fact.

[1] Supported in part by grants from "Stem 2001" from Ministero della Salute, Fondi per gli Investimenti della Ricerca di Base (FIRB) (RBNE019J9W), and "Progetto Genomica Funzionale" from Ministero dell'Istruzione dell'Università e della Ricerca (MIUR) (to P. V.) and FIRB (RBNE01RNN7; to A. M.). hBUB1 rabbit antibody was a kind gift of T. Yen (Fox Chase Cancer Institute, Philadelphia, PA). A. Musio is a fellow of Associazione Rimini Genoma Onlus.

[2] To whom requests for reprints should be addressed, at Istituto di Tecnologie Biomediche, Consiglio Nazionale delle Ricerche, Via Fratelli Cervi, 93, 20090 Segrate, Milan, Italy. Phone: 39 02 26422632; Fax: 39 02 26422660; E-mail: antonio.musio@itb.cnr.it.

[3] The abbreviations used are: CIN, chromosome instability; MIN, microsatellite instability; AI, anchorage-independent; CGH, comparative genomic hybridization; SKY, spectral karyotyping; MMC, mitomycin C; siRNA, small interfering RNA; RT-PCR, reverse transcription-PCR; FISH, fluorescence *in situ* hybridization; TUNEL, terminal deoxynucleotidyltransferase-mediated dUTP nick end labeling.

doubling was calculated as $\log_2 (D/D_0)$, where D is the density of cell when harvesting, and D_0 is the density of cells when seeding. Senescence occurred at estimated population doublings of 64–69. At this stage, cells failed to reach confluence despite regular refeeding, and they showed the characteristic unlarged, flattened shape of senescent cells. In addition to these parameters, both molecular and biochemical markers were investigated (see below). In addition, a second cell line (subject 2), established from a Caucasian woman, was used for antisense inhibition studies only.

Antisense Oligonucleotide Methodology. The general experimental approach to antisense has been described (20). For inhibition studies, three oligodeoxynucleotides were synthesized (sequences available on request): (*a*) antisense oligomer designed as a complementary sequence at the 5′ end of the coding region; (*b*) sense oligomer from the identical region; and (*c*) scrambled oligomer with the same nucleotides used for the antisense oligomer. We performed two different protocols with antisense oligonucleotide treatment: (*a*) short term and (*b*) long term. In short-term culture, cells were treated with 40 μg/ml each antisense, sense, and scrambled oligonucleotides (diluted in DMEM) for 24 h and an additional 20 μg/ml for another 24 h. In long-term culture, after the first treatment with 40 μg/ml, cells were treated with 20 μg/ml each antisense, sense, and scrambled oligonucleotides for an additional 8 days. In addition, mock controls, by adding DMEM without oligonucletides, was performed.

Ribozyme Design, Synthesis, and Treatment. The ribozyme design was performed according to an original approach, which makes use of a computer method for the analysis of target mRNA sequences (21). A series of ribozyme sequences were correspondingly deduced. The final analysis accounting for the correct structure activity relationship enabled us to select the hammerhead ribozyme addressed to AUA triplet located at the 2711 position on the coding region of *BUB1* mRNA. The ribozyme sequence is: 5′-CAGGGGCUGAUGAGGCCGAAAGGCCGAAAUUUUUAUAGA-3′(*Rz-BUB1*). In addition to the active form of *Rz-BUB1*, a mutated catalytically inactive ribozyme sequence was synthesized (*inact-Rz-BUB1*) carrying the mutation $G_5 > A_5$ in the active core. *Rz-BUB1* and *inact-Rz-BUB1* were synthesized by introducing chemical modifications conferring resistance to RNase A, as described previously (22). At the end, the crude product was processed and purified as already described (23). Ribozyme was purified maintaining sterile RNase-free conditions in a MonoQ-HR 16/10 (Amersham Pharmacia Biotech) strong ion-exchange high-performance liquid chromatography preparative chromatography. For culture treatment, 1 μM *Rz-BUB1* or *inact-Rz-BUB1* was added to cell culture for 48 h.

siRNA Synthesis and Cell Treatment. siRNA corresponding to *BUB1* mRNAs was designed as recommended (24) with two base overhangs (Xeragon). The following gene-specific sequence was used: si-BUB1 5′-CAUCACUUUUUCAGGGGUA dTT-3′. Cells (at 40–60% confluence) were transfected with 200 nM si-*BUB1* RNA by using Oligofectamine Reagent (Invitrogen). Cells were analyzed for aneuploidy frequency 48-h post-transfection.

Immunoprecipitation and Western Blots. Analysis with p21, p53 (Santa Cruz Biotechnology), SMC1 (Bethyl), and BUB1 (a rabbit polyclonal antibody; a kind gift of T. Yen, Fox Chase Cancer Institute, Philadelphia, PA) antibodies was performed according to a published protocol (25). Briefly, specific antibody was incubated at 4°C with protein extracts for 1 h. Protein A-agarose (Santa Cruz Biotechnology) was added overnight, followed by four washings with buffer lysis. Samples were boiled in sample buffer and separated by SDS-PAGE. The proteins were transferred to nitrocellulose membrane (Amersham) and incubated with primary antibody (1:250–1:2000 dilution). After removal of the unbound primary antibody, membranes were incubated with secondary antibody-peroxidase conjugate (Sigma), processed for detection by chemiluminescence (Amersham), and imaged on Biomax film (Kodak). Actin and tubulin antibodies (Santa Cruz Biotechnology) were used as internal controls.

ARP1 Expression by RT-PCR Analysis. Total RNA was extracted from cells exposed to ARP1 antisense oligonucleotides by the SV Total RNA Isolation System (Promega) and used for cDNA synthesis with random hexamers. The following primers were used to amplify ARP1 cDNA (spanning from exon 1 to 6): Arp1-F: TGT CGT GAT CGA CAA CGG AT, ARP1-R: AAG TCG TAG CCC TCC TTA C. The presence of ARP1 transcripts was analyzed by PCR performed combining both a variable number of amplification cycles and different dilutions of primers. Hypoxanthine phosphoribosyltransferase was used as internal standard.

Cytogenetic Analysis. Exponentially growing fibroblasts were treated with colcemid (0.05 μg/ml; Life Technologies, Inc.), harvested, incubated with 0.075 M KCl, and fixed in methanol:acetic acid 3:1. Chromosome preparations were G-banded according to the trypsin digestion procedure, and aneuploidy cells, *i.e.*, any variation from diploid number, were scored by direct microscopic examination.

Assays for Mutation to Ouabain and 6-Thioguanine Resistance. Control and antisense-treated cells were seeded at 10^5 cells into 100-mm dishes and at 200 cells into 60-mm dishes to determine the plating efficiency. Twenty-four hours later, either ouabain (Sigma), at a concentration of 1 μM, or 6-thioguanine (Sigma), at a concentration of 3×10^{-5} M, was added to the 100-mm dishes to determine the number of resistant colonies. Mutant colonies were fixed, stained, and scored 3 weeks after the initial seeding. The mutation frequency was calculated as: (resistant colonies)/(cells seeded × S), where S is the plating efficiency of cells.

MMC Treatment. AI clones were treated with MMC (30 μM, diluted in PBS; Sigma) or with an equivalent amount of PBS for 24 h.

Soft Agar Assay. Cells were suspended in 3 ml of 0.3% agar (Difco) supplemented with complete growth medium. This cell suspension was allowed to solidify at room temperature on 4 ml of a 0.5% agar base layer containing growth medium in 60-mm dishes.

FISH. *In situ* hybridization with a biotin-labeled probe recognizing all of the human centromeres (Appligene Oncor) was performed according to a published protocol (26). DNA was counterstained with 0.1 μg/ml propidium iodide.

SKY. SKY was performed as described (27). After *in situ* hybridization, images were acquired using an epifluorescence microscope (DMRXA; Leica) connected to an imaging interferometer (SD200; Applied Spectral Imaging) and analyzed using SKYView v1.6 software (Applied Spectral Imaging). Six to 10 metaphases were analyzed for each cell line.

CGH. For CGH, DNA was prepared using high salt extraction and phenol purification and labeled by nick translation using biotin-11-dUTP (Roche). Biotin-labeled DNA and digoxigenin-labeled normal donor DNA (sex matched) was cohybridized to sex-matched normal human lymphocyte metaphase chromosomes. Images were acquired with a Leica DMRXA epifluorescence microscope (Leica) using fluorochrome-specific filters (Chroma Technologies). Quantitative fluorescence imaging and CGH analysis was performed using Leica CW4000CGH software (Leica Microsystem Imaging Solutions).

Immunohistochemistry. Cells were cultured on chamber slides (Falcon), washed in PBS, fixed with ice-cold methanol for 10 min, and washed again in PBS. Incubation with a monoclonal anti-γ-tubulin antibody (Sigma) diluted 1:1000 in 3% goat serum/PBS was performed overnight at 37°C. The antibody complexes were detected with tetramethylrhodamine isothiocyanate-conjugated goat antirabbit IgG (Sigma) and counterstained with 4′,6-diamidino-2-phenylindole. Gray level images were acquired using a charged-couple device camera (CH250; Photometrics) mounted on a Leica DMRXA epifluorescence microscope and pseudo-colored using Leica Q-Fish software. Five hundred cells were analyzed for each cell line. Additional details for CGH, SKY, and immunohistochemistry protocols can be found on the Internet.[4]

Apoptosis Assay. TUNEL assay for DNA fragmentation was done using an "*In Situ* Death Detection" kit (Roche) according to manufacturer's recommendations.

Sequencing of p53 and BUB1. Both p53 and BUB1 coding region were amplified by RT-PCR and directly sequenced. Total RNA was extracted by SV Total RNA Isolation System (Promega) and used for cDNA synthesis with random hexamers. The RT-PCR products were purified on an agarose gel and sequenced using Thermosequenase (Amersham).

Telomerase Assay. Cellular extracts were assayed for telomerase activity with a PCR-based telomeric repeat amplification protocol (TRAPeze kit; Intergen) assay. PCR products were electrophoresed on 10% polyacrylamide gel and stained with silver staining kit (Amersham).

Tumorigenicity Assay. Cells were trypsinized, resuspended in PBS, and inoculated s.c. in nude mice (Charles River Breeding Laboratories) at a

[4] Internet address: http://www.riedlab.nci.nih.gov/.

concentration of 3×10^6 in 0.3 ml. As positive control, human Kaposi's sarcoma cells were injected s.c. in nude mice at the same concentration. At least three mice for each cell line were injected, and mice were followed ≤2 months to allow cell growth. At the end of this period, or when tumor mass reached ~0.5 cm^3, animals were sacrificed, and completed necropsy was performed.

RESULTS

Chromosome Abnormalities Arise in Fibroblasts through Inhibition of Genes Involved in Mitosis. We chose to use antisense-mediated transcriptional inhibition to query the respective roles of 13 genes known to be involved in chromosome condensation (*SMC1*), kinetochore assembly (*CENP-A, -B, - C, -E,* and *-F*), the spindle checkpoint (*BUB1, BUB3, MAD2, INCENP, INTZW10,* and *ZW10*) and spindle formation (*ARP1*) with respect to chromosome segregation fidelity.

Primary human fibroblasts at passage 4 were mock treated or treated with each of these antisense and control oligonucleotides, which include both sense and scrambled oligonucleotides, and thereafter, the effect on correct chromosome segregation was evaluated by analysis of chromosome number, the presence of micronuclei, and apoptosis.

As shown in Table 1, antisense oligonucleotides directed against 9 of the 13 genes induced chromosome aneuploidy, although to a different extent. Inhibition of genes coding for *SMC1, ARP1,* and those involved in the formation of the mitotic spindle or its checkpoint (*BUB1, BUB3,CENP-E, MAD2, INCENP, ZW10,* and *INTZW10*) had a high, statistically significant number of aneuploid mitoses. In fact, the frequency of aneuploid cells ranges from 15% with *BUB1* to 26% with *BUB3* and *SMC1* antisense oligonucleotides when compared with 2% in control cells. With the exception of CENP-B, very similar results were obtained when antisense inhibition was performed on a second human fibroblast cell line. However, treatments with *CENP-A, CENP-C,* and *CENP-F* antisense oligonucleotides resulted only in a slight increase in aneuploid cells. As the aim of our preliminary experiments was to perform a screening for the identification of genes giving rise to aneuploidy, we did not further investigate whether the results obtained with the four *CENP* family genes reflected a nonessential role in the maintenance of genome integrity or whether they were attributable to a failure of the antisense technology. Interestingly, the identification of putative genes conferring CIN will allow to test a recent mathematical model developed to study the effect of CIN on the evolution of cancer (28). Treatment with *SMC1* antisense oligonucleotide, besides aneuploidy, also induced chromosome aberrations in 20% (subject 1) and 22% (subject 2) of the cells (Table 1), including gaps, whereas breaks were very rare. These data are consistent with the role of SMC proteins, which contribute to both condensin and cohesin complexes and with the phenotype of *smc* mutants in yeast, which show an increased rate of aneuploidy, defects in nuclear division, and partial chromosome decondensation (29).

Table 1 *Percentage of aneuploid cells after oligonucleotide antisense treatments*

	Subject 1		Subject 2	
	Aneuploidy cells	Chromosome aberrations	Aneuploidy cells	Chromosome aberrations
Control	2	2[a]	4	3
ARP1	24	3	31	4
BUB1	15	3	12	4
BUB3	26	2	27	6
CENP-A	3	2	4	2
CENP-B	4	4	18	5
CENP-C	3	2	5	5
CENP-E	21	3	21	4
CENP-F	5	4	3	2
INCENP	20	4	23	5
INTZW10	22	6	18	7
MAD2	20	3	31	4
SMC1	26	20	31	22
ZW10	17	4	27	5

[a] Gaps and breaks.

To further substantiate the mechanism of formation of aneuploid cells, we performed additional cytogenetic investigations. Abnormalities in the segregation process result in micronuclei and anaphase bridge formation. Cells treated with aneuploidy-causing antisense oligonucleotides were analyzed for the presence of micronuclei (Fig. 1, *A* and *B*). All these cell cultures showed a variable but increased number of micronuclei when compared with controls as shown in Fig. 2*A*. *ZW10* antisense-treated cells had the highest number (17%) of cells with micronuclei, followed by *INTZW10* (10%), *INCENP* (9%), and *BUB3* (9%) antisense-treated cells. Treatments with antisense against the other genes gave only a slight increase when compared with the baseline level of 3% observed in control cells. Additional defects observed in antisense-treated cells included occasional nuclear bridges. When FISH was performed using a pancentromeric probe, the micronuclei contained at least one centromere signal (Fig. 1, *C* and *D*), providing evidence that the micronuclei represented lagging chromosomes attributable to mis-segregation.

Most cells respond to defects in chromosome segregation by activating apoptotic programs. To investigate whether mis-segregation triggers apoptosis in our system, we performed TUNEL assay on cells treated with antisense oligonucleotides (Fig. 1, *E* and *F*). All treatments, except *CENP-A, CENP-B, CENP-C,* and *CENP-F* antisense oligonucleotides, induced massive apoptosis ranging from 25% with *ZW10* and *MAD2* to 13% with *INCENP* (Fig. 2*B*). In contrast, control cells had only 3% of apoptotic cells. Thus, the high incidence of aneuploid cells correlates with an increase in apoptotic rate and micronuclei formation, suggesting that most aneuploid cells undergo elimination by programmed cell death.

Effect of *ARP1, BUB1,* and *SMC1* Antisense Oligonucleotide Treatments on Long-term Cell Cultures. As reported above, abnormal chromosome segregation leads to apoptosis, although its effects on long-term cultures have not been evaluated *in vitro*. Indeed, some cells with altered chromosome number could escape programmed death, and their fate is unknown. To investigate this point, we started long-term cultures of three antisense treated cells, *ARP1, BUB1,* and *SMC1,* according to an experimental protocol outlined in Fig. 3. These genes were selected because they are thought to damage normal mitosis through different mechanisms, yet caused significant aneuploidy in our short-term test (Table 1). In addition, *BUB1* has already been shown to be involved in human tumorigenesis (30). Fibroblast cells were treated for 9 days with antisense oligonucleotides and subsequently cultured as usual. With this protocol, a down-regulation of BUB1 and SMC1 protein synthesis was obtained, as shown by Western blotting with specific antibodies (Fig. 4, *A* and *B*). Reduction of the levels of ARP1 transcripts was investigated by RT-PCR, because by reducing primer concentration, a specific ARP1 band was seen only in control cells (Fig. 4*C*).

Aliquot analysis of cell cultures was performed at the 5th day and at the end of the treatment (2 and 4 days after). High frequency of aneuploidy was confirmed in treated cells when compared with the untreated counterpart, as well as to the control oligonucleotide-treated cells. The frequency of apoptotic cells ranged from 32% (with *BUB1*) to 44% (with *SMC1*), whereas control cultures had very few apoptotic cells ranging from 2 to 4% (Fig. 2*C*). Apoptosis correlated with the frequency of micronuclei (Fig. 2*D*) and the number of apoptotic cells and remained elevated even 4 days after the treatment was discontinued. In these experimental conditions, *SMC1* antisense oligonucleotide treatment induced the highest level of micronuclei and apoptotic

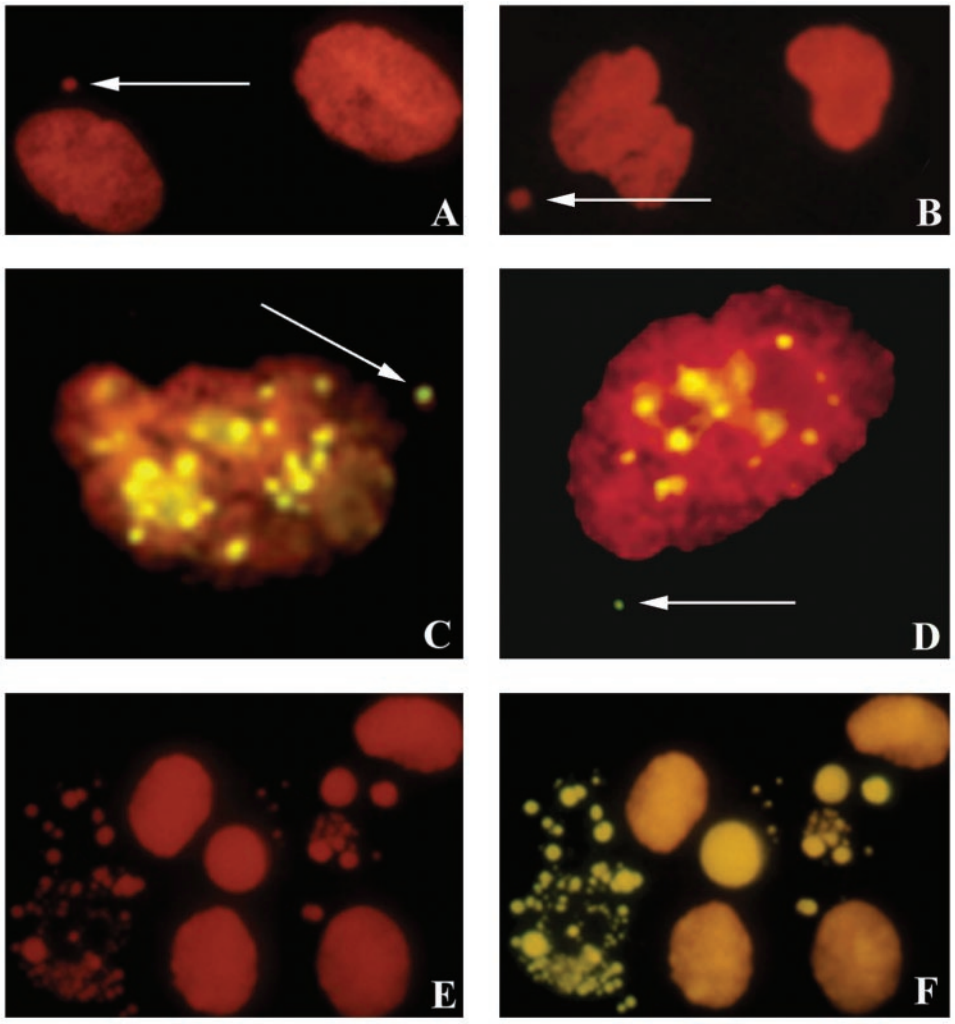

Fig. 1. Effects of antisense treatments on fibroblast cells. Antisense treatments lead to micronuclei formation (*A*, *B*, *arrows*), which, as shown by FISH performed with a probe hybridizing to all human centromeres, contain at least one chromosome (*C*, *D*, *arrows*). Typical apoptotic bodies stained by propidium iodide (*E*); they show an intense fluorescence when TUNEL assay was performed on the same sample (*F*), indicating that a massive DNA fragmentation occurred.

cells when compared with *ARP1* and *BUB1*. The presence of chromosomes in micronuclei was also confirmed by FISH (data not shown).

To investigate whether, as a consequence of aneuploidy, a few cells could acquire AI growth features, we assessed the ability of cells to grow in soft agar. At the 25th passage, *BUB1* antisense oligonucleotide-treated cells were able to form colonies in soft agar, whereas no colony was found in *ARP1*- and *SMC1*-treated and control cells. The colonies were transferred to standard culture conditions and are still in culture (passage 63).

Investigation of Consequences of *BUB1* Inhibition. Inhibition of a specific function by antisense technology needs to be thoroughly substantiated. In addition, although human fibroblasts usually do not give rise to AI colonies, a single clone could have arisen by chance. To exclude this possibility, we used alternative approaches to modify gene transcription by treating fibroblasts both with a specific ribozyme and by siRNA in the short-term assay (for 48 h, see "Materials and Methods") and counted aneuploid cells. As a matter of fact, 58.8% with ribozyme and 35% with siRNA of cells were aneuploid, whereas untreated or control ribozyme and siRNA-treated cultures showed the normal rate of aneuploidy (2–4%), thus confirming the specificity of the antisense results. These treatments do not cause BUB1 abnormality, because sequencing of this gene in three AI clones did not detect any mutation.

As stated above, inhibition of *BUB1* expression at the protein level by Western blot was shown to occur in antisense-treated cells collected 9 days after the exposure to oligonucleotides. These data were also confirmed by a time course experiment where BUB1 synthesis was analyzed at different times during antisense treatment. In this experiment, specific bands were evident after 6 and 12 h of treatment but not after 24 and 48 h (Fig. 4*D*), whereas actin protein levels were unaffected. As actin is degraded during apoptosis (31), these results suggest that BUB1 inhibition is specific and not caused by aspecific degradation triggered by apoptotic events.

To confirm that inhibition of *BUB1* function occurred in fibroblasts, we investigated whether the spindle checkpoint, in which *BUB1* plays a fundamental role, is abrogated in antisense-treated cells. Antisense-treated cells were exposed to the spindle-destabilizing agent nocodazole, and their mitotic index was recorded. Consistent with the loss of spindle checkpoint, *BUB1* antisense oligonucleotide-treated cells showed no peak at any time, whereas a peak at 18 h was seen in all control populations (Fig. 4*E*).

To confirm that antisense treatment can give rise to clones with an AI phenotype, we repeated the experiments with five independent fibroblast cultures. Two independent clones growing in soft agar were identified in antisense-treated cultures, whereas no growth was seen in soft agar plates, where untreated and control oligonucleotide-treated cells were seeded. These two clones were transferred to standard culture conditions and are still growing. All together, the frequency of anchorage independence after antisense treatment was $\sim 1.5 \times 10^{-6}$ (in still ongoing experiments performed with ribozyme-treated cultures, the estimated frequency was 3×10^{-6}; data not shown).

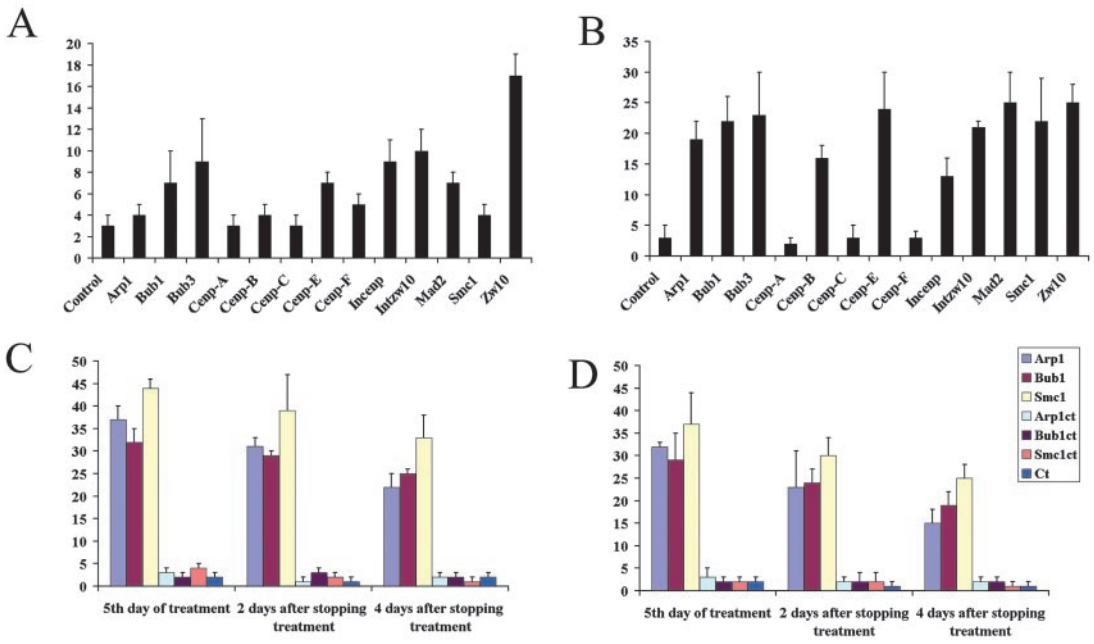

Fig. 2. Effect of antisense oligonucleotides in short- and long-term treatments. Micronuclei (*A*) and apoptosis (*B*) frequencies in human fibroblasts exposed to *ARP1*, *BUB1*, *BUB3*, *CENP-A*, *-B*, *- C*, *-E*, *-F*, *INCENP*, *INTZW10*, *MAD2*, *SMC1*, and *ZW10* antisense oligonucleotides. Effect of *ARP1*, *BUB1*, and *SMC1* antisense on human fibroblasts at 5th day of treatment and 2 and 4 days after long-term treatment (see "Materials and Methods" for details). Frequency of apoptosis (*C*) and micronuclei (*D*) obtained with *ARP1*, *BUB1*, and *SMC1* antisense-treated and control cells. Because no significant difference among mock buffer-treated, sense, and scrambled oligonucleotide-treated cells was found, these data have been pooled. At least 500 cells were analyzed for micronuclei and apoptosis for each individual treatment. Average and error standard are based on two independent experiments.

Cytogenetic and Molecular Analysis of Polyclonal and Clonal Fibroblast Cells. Karyotype analysis by G banding of untreated and *BUB1* antisense-treated fibroblasts was performed during *in vitro* cultures at various passages. Although untreated and control oligonucleotide-treated cells showed a low percentage of aneuploid cells, fibroblasts treated with *BUB1* antisense show aneuploidy (8%, compared with 1–2% of the other populations). Apparently, temporary inhibition of *BUB1* is sufficient to confer an aneuploid phenotype that persists in culture. However, no recurrent chromosomal abnormality was identified.

Aneuploidy was also detected in the three AI clones, which were also investigated by SKY and CGH. SKY analysis showed no chromosome rearrangements, *i.e.*, chromosome translocations or other structural defects, in AI clones (Fig. 5*A*). Moreover, the analysis of 22 metaphases showed a widespread variability in chromosome number that range from 36 to 74 with a predominance of chromosome losses. SKY analysis of individual AI clones suggests specific chromosome aneuploidy, such as the recurring loss of chromosome 6 in 5 of 8 metaphases in clone 1 and loss of chromosome 21 in 4 of 6 metaphases in clone 2. This finding, however, could not be corroborated with CGH analysis, because the results essentially revealed a balanced genome (Fig. 5*B*). CGH can detect imbalances when present in >50% of the cells. Taken together, these data suggest that the development of AI phenotype is not attributable to specific chromosome rearrangements but that the acquisition of the AI phenotype is accompanied by a manifestation of genome instability of the chromosomal type (CIN). A selection for specific chromosomal aneuploidies, as observed in cancer cells, has not yet occurred.

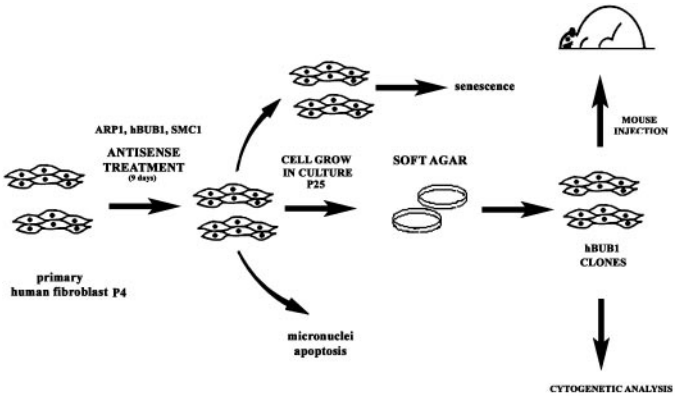

Fig. 3. Flow chart describing the experimental protocol. Human fibroblasts at passage 4 were treated for 9 days with *ARP1*, *BUB1*, and *SMC1* antisense oligonucleotides with adequate controls. Alterations in chromosome segregation induced by treatments led to micronuclei formation and apoptosis. After removing oligonucleotides, fibroblasts were cultured and tested at different passages during *in vitro* progression for chromosome number, presence of chromosome aberrations by G banding, and capability to growth in soft agar. At passage 25, one clone, derived from *BUB1*-treated cells, acquired AI phenotype, whereas no clones were obtained from *ARP1*- and *SMC1*-treated and control cells. Two additional AI clones were obtained in a second independent experiment. These clones are continuously growing *in vitro*, whereas control cells and antisense polyclonal-treated cells are senescent. The last step of our protocol was the evaluation of tumorigenicity of AI clones by inoculation in nude mice.

Senescence, CIN, and Tumorigenesis. Polyclonal fibroblasts, both untreated and treated, and the AI clonal populations were cultured with standard protocols to evaluate whether they maintain the senescent phenotype, which usually occurs with human normal fibroblasts. All of the polyclonal and clonal populations were tested at the 44th passage. Cell cycle arrest and senescence are associated with molecular markers, such as p21. An accumulation of p21 was found in polyclonal populations in contrast to a very faint band in AI clones (Fig. 6*A*), providing evidence that AI clones have not yet reached a senescent stage, whereas control and antisense oligonucleotide-treated cells did so. Senescent polyclonal populations (passage 44) showed no specific chromosome aneuploidy when analyzed by CGH, whereas the level of micronuclei and apoptosis was very low (0.2%), in agreement with published data on senescent cells (32).

Because the abrogation of replicative senescence has been related to telomerase expression, we investigated whether polyclonal and clonal populations showed detectable activity of the catalytic component of telomerase, *hTERT*, by the TRAPeze assay. Telomerase ac-

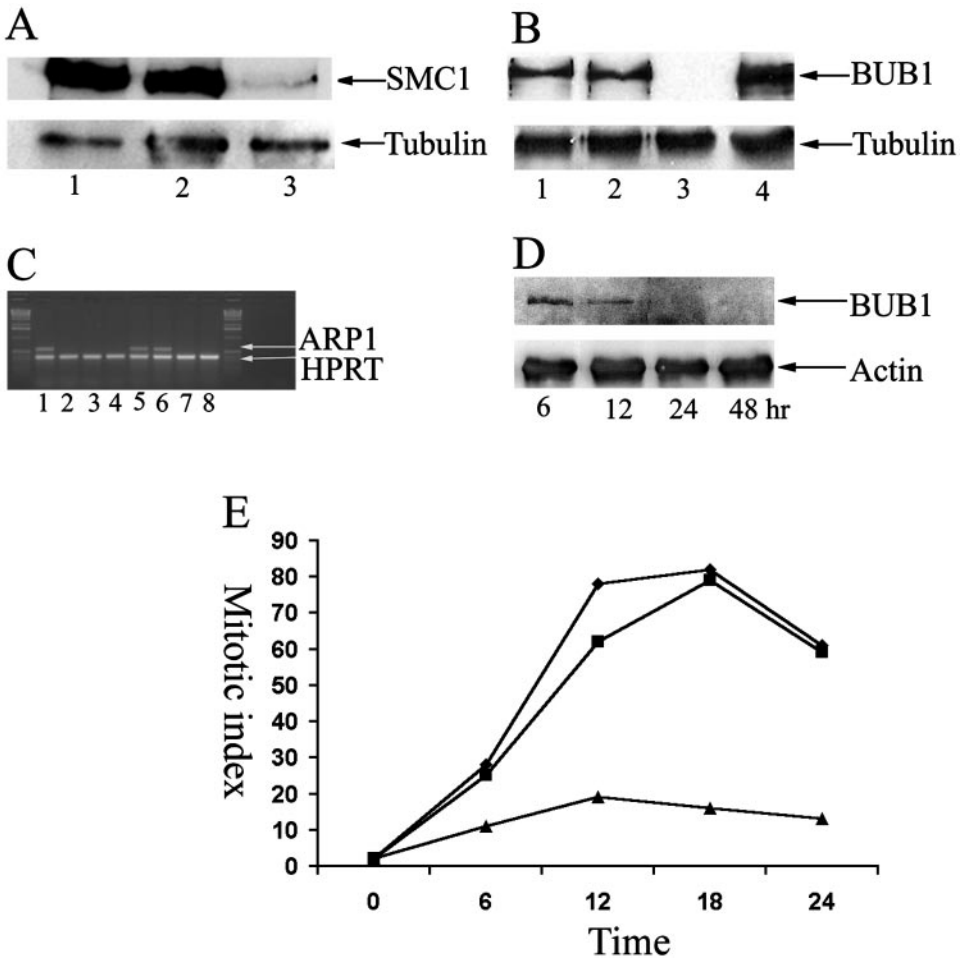

Fig. 4. Effect of antisense oligonucleotide treatment on SMC1, ARP1, and BUB1 expression. Western blot with SMC1 and tubulin-specific antibodies (*A*) performed on untreated (*Lane 1*), scrambled control oligonucleotide-treated (*Lane 2*), and SMC1 antisense-treated cells (*Lane 3*). Western blot with BUB1 and tubulin-specific antibodies (*B*) performed on control untreated cells (*Lane 1*), control oligonucleotide-treated cells (*Lane 2*), antisense-treated cells (*Lane 3*), and HeLa cells used as positive control (*Lane 4*). RT-PCR (*C*) performed, with decreasing concentrations of primers, on cells treated with ARP1 antisense oligonucleotide (*Lanes 1–4*) and control cells (*Lanes 5–8*). Time course inhibition of BUB1 protein (*D*). Effect of nocodazole exposure on mitotic index in untreated (♦), control oligonucleotide (■), and antisense-treated cells (▲; *E*).

tivity was detected neither in polyclonal fibroblasts nor in AI clones, whereas a clear ladder was present in positive control and HeLa cells (Fig. 7*A*).

Although the molecular basis of CIN is still unknown, it has been suggested to result from various mechanisms, including p53 deregulation or mutations. A p53 function study was performed. After MMC treatment, p53 was up-regulated in all AI clones, and this led to an up-regulation of p21 (Fig. 6*B*), suggesting that in AI clones, p53 function is maintained. Moreover, no mutations were found in AI clones by sequencing the entire protein coding region of the *p53* gene (data not shown). This is consistent with the consideration that antisense oligonucleotide treatment does not induce nucleotide mutations. Furthermore, we found no significant increase in either ouabain or 6-thioguanine resistance of AI cells, because the number of colonies growing in selective media did not appreciably vary when compared with control cells (0.2 *versus* 0.33×10^{-6} cells for ouabain and 1 *versus* 1.4×10^{-6} cells for 6-thioguanine resistance). These values are in agreement with the frequencies reported for normal cells (33, 34), suggesting that *BUB1* is not involved in specific processes that prevent the formation of mutations at nucleotide levels.

Another mechanism which has been suggested to lead to CIN is the presence of centrosome abnormalities (17). To further investigate this possibility, centrosomes were visualized microscopically by labeling the cells with antibody against γ-tubulin. In both AI clones and polyclonal fibroblasts, centrosomes had visible, clearly defined, dot-shaped structures (Fig. 7, *B* and *C*), and the number of cells with abnormal centrosomes was similar in all populations (data not shown). It is, however, important to note that these cells have not yet acquired a neoplastic phenotype, because they were unable to grow when injected s.c. in nude mice (data not shown).

DISCUSSION

Proliferation, differentiation, senescence, and tumorigenesis are linked through complex pathways of gene expression, which in recent years have become amenable to both *in vitro* and *in vivo* studies. The availability of transgenic and knockout mice has provided new tools to dissect the various metabolic pathways whose alterations contribute to neoplastic transformation. These studies have been instrumental to form our current vision of tumorigenesis as being the result of multiple independent genetic changes, which include oncogene activation, tumor suppressor inactivation, epigenetic changes, and whole genome abnormalities (6).

Although extremely interesting, data acquired in rodents cannot necessarily be transferred to humans. Differences exist between these species (5), and the data obtained in mice must be independently corroborated by human studies. To accomplish this task, most of the approaches have investigated the growth potential of cells cultured *in vitro*. Historically, fibroblast cells have been the tissue of choice (35). Fundamental studies have suggested that human fibroblast cells have a limited life span (Hayflick limit) and that, different from rodent cells, the rate of spontaneous transformation is considerably lower. This proliferative block, which is thought to represent a genetic guard to neoplastic transformation (36), is at least in part related to the loss of the ability to faithfully replicate telomeric ends (37, 38). Human fibroblasts transfected with the catalytic subunit of telomerase are

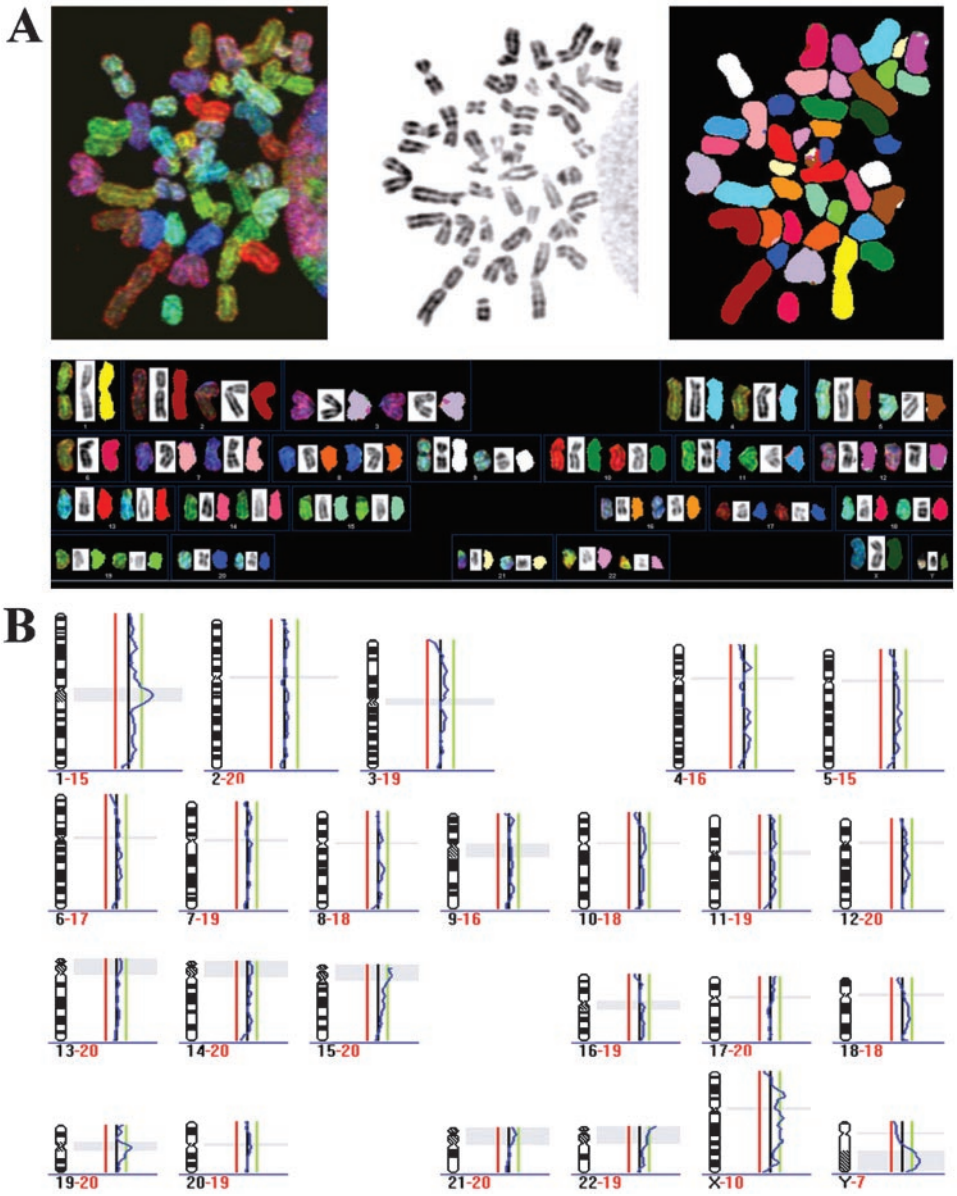

Fig. 5. Molecular cytogenetic characterization of AI clones. SKY analysis of AI clone 1. In this particular cell, loss of chromosomes 1 and 6 is shown (*A*). Representative CGH analysis of AI clone 1 (*B*).

immortalized, growing continuously *in vitro*, but are not aneuploid, do not acquire AI ability, and do not grow in nude mice (19, 38, 39). Additional genetic changes are needed to confer the complete neoplastic phenotype to fibroblasts (4).

Most solid tumors are aneuploid (40), yet aneuploidy is rarely found in normal cells. It is generally believed that aneuploidy in normal cells is commonly followed by apoptosis. However, the possibility exists that these aneuploid cells can escape apoptosis and show a selective growth advantage, which could represent the substrate to achieve additional genetic changes. In this case, although being insufficient for acquisition of complete tumoral phenotype, aneuploidy could be a very early step in transformation. To investigate the role of aneuploidy in tumorigenesis has been difficult even in the mouse model because animals in which several genes interfering with normal chromosome segregation have been inactivated often die *in utero* because of profound derangement of normal cellular replication (41). However, it has recently been shown that haploinsufficiency in *Mad2* spindle checkpoint gene in mice gives rise to chromosomal instability and high lung tumor incidence (42). This suggests that aneuploidy

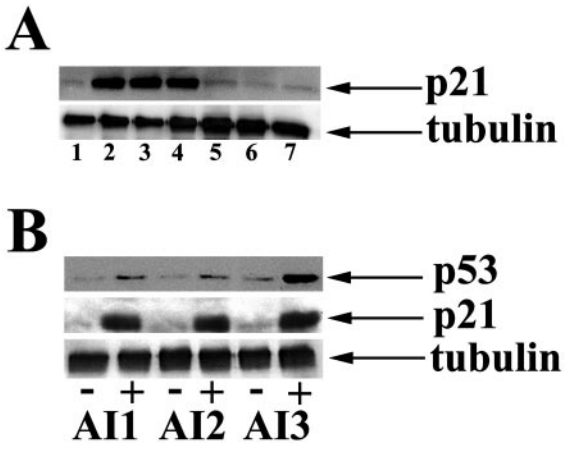

Fig. 6. Molecular marker of senescence and p53 function. Western blot of p21 (*A*) performed on primary cells (*Lane 1*), senescent untreated cells (*Lane 2*), senescent scrambled oligonucleotide-treated cells (*Lane 3*), senescent antisense oligonucleotide-treated cells (*Lane 4*), and AI clones (*Lanes 5–7*). Western blot of p53 and p21 (*B*) performed on untreated (−) and MMC-treated AI clones (+).

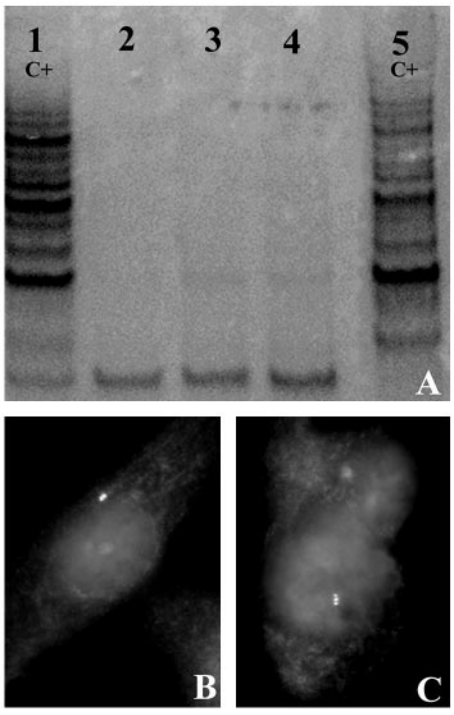

Fig. 7. Characterization of AI clones. Telomerase activity analysis by TRAPeze assay of AI clones (*A*). A typical ladder is present in control cells provided by the manufacturer (*Lane 1*) and in HeLa cells, an additional positive control (*Lane 5*), but not in the three AI clones (*Lanes 2–4*). Centrosome number was evaluated by scoring γ-tubulin signals within a single cell: most cells show centrosome stability, *i.e.*, one or two dots (*B*), whereas occasionally, altered centrosome number (>2) was detected (*C*).

could play a role in the early phase of transformation at least in rodent cells.

To investigate whether aneuploidy could play a role also in early tumorigenesis in humans, we set up a gene inhibition system in human fibroblasts. Both senescence and transformation have been extensively studied in this model, and many correlations between these two processes have been identified. We reasoned that by interfering with chromosome segregation, we could obtain aneuploid cells without causing any concomitant DNA damage at the sequence level and that the fate of these cells could then be followed *in vitro* by direct analysis of cultured cells. Inhibition by antisense technology, however, must be strongly corroborated. We think that our approach achieved substantial inhibition of *BUB1* function for the following reasons: (*a*) the same pattern of aneuploidy without chromosome breakage, consistent with the known *BUB1* role in spindle checkpoint, was obtained in 13 independent experiments, using both antisense oligonucleotides and ribozyme but not with control oligonucleotides; the greater number of aneuploid cells obtained with ribozyme could be attributable to a stronger inhibition usually associated with the ribozyme technique compared with the oligonucleotide approach; (*b*) similar results were also obtained with the use of the siRNA approach, a new technology for inhibition of gene expression; (*c*) using an antibody against BUB1, no protein was immunoprecipitated in antisense-treated cells after 24 h of treatment, and its disappearance followed a decrease after 6 and 12 h; and (*d*) nocodazole exposure performed during treatment with antisense showed loss of the ability of treated cells to stop the mitotic process, demonstrating functional inactivation of the spindle checkpoint.

For all these reasons, we think that the effects found in our cell cultures reported in the present study can be directly related to a substantial interference with the function of *BUB1* in spindle checkpoint. With this approach, we were able to demonstrate that aneuploidy can have different effects on the fate of the cells. As shown by our data, most aneuploid cells undergo apoptosis, but a substantial portion of them are able to survive without profound alterations in their proliferative potential and still able to senesce at the appropriate time, suggesting that the genetic program leading to senescence in normal fibroblast is not automatically altered in aneuploidy. However, our data raise the possibility that with rare frequencies, aneuploid cells could acquire different proliferative abilities that confer to them the ability to grow without anchorage dependence and postpone their senescence.

Delayed senescence of human fibroblasts has been achieved by exogenous telomerase expression. In mice, several genes, including *p53*, are known to play a role in replicative or Ras-induced senescence. However, our analysis did neither find abnormalities in p53 nor telomerase activity, although we cannot exclude a telomerase-independent alternative lengthening of telomeres. These data would suggest that the mechanisms leading to the insurgence of AI clones are different from those involving these genes. Likewise, centrosome abnormalities were absent in most cells, suggesting that they are not responsible for chromosomal instability in our system. However, we cannot exclude the formal possibility that mutations in other genes contributed to the acquisition of AI phenotype, although we think that this is unlikely in view of the results obtained in oubain and thioguanine resistance experiments.

The clones identified here have some features reminiscent of CIN. Theoretically, temporary inhibition of spindle checkpoint could allow the insurgence of chromosome instability, but the cells should switch to a stable aneuploid state when *BUB1* activity is restored. The reason why this does not occur in our clones is not clear at the moment, but it could be that, by escaping the checkpoint for several mitoses, the cells could become insensitive to the restoration of the checkpoint. The mechanisms underlying this phenomenon need to be further investigated.

CIN could be the first determinant of neoplastic transformation, allowing different combinations of chromosomes to take place, therefore providing a substrate for further selection on the basis of small growth advantage based on a specific set of chromosome content. Alternatively, CIN could be a late event in cancer pathogenesis, representing a stage in which all of the checkpoints have been inactivated and mitoses proceed completely abnormally. Our finding that both the antisense-treated aneuploid polyclonal fibroblast population and the three AI clones present a largely variable chromosome content suggests that CIN, in selected situations, could be an early event in cell transformation. A likely possibility at this point is that both mutations and aneuploidy could be the first event in the multistep process leading to cancer.

In colon cancer, CIN appears to be mutually exclusive with MIN. Thus far, despite many investigations, although genes responsible for MIN have been identified, no germ-line inactivation of spindle checkpoint genes has been identified in human cancer (15). In addition, most colon cancers with CIN appear to be sporadic and not related to familial cancer syndromes. We demonstrate here that temporary inactivation of checkpoint is sufficient for CIN to occur in cultured cells and that this characteristic is maintained after the toxic insult has been eliminated. Interference with normal spindle checkpoint can be caused by many toxic agents, which can be found in diet or are endogenously produced in the colonic mucosa. The possibility exists that, although MIN is mainly of genetic origin, CIN arises in colon cells after environmental-driven, temporary inhibition of normal gene function. CIN could then provide few cells a peculiar chromosome content, allowing a small but sufficient growth advantage, which could be the substrate for additional genetic and/or epigenetic changes. Interest-

ingly, this "hit-and-run" mechanism of genetic interference would leave no signature, which could be identified by genetic analysis.

ACKNOWLEDGMENTS

We thank Prof. A. Albertini for encouragement. We also thank L. Susani and M. Mirolo for their technical assistance. Finally, we thank T. Mariani (Istituto di Biofisica, Consiglio Nazionale delle Ricerche, Pisa, Italy) for statistical analysis.

REFERENCES

1. Boveri, T. (ed.). Zur Frage der Entstehung Maligner Tumoren, pp. 1–64. Jena: Gustav Fisher, 1914.
2. Cahill, D. P., Kinzler, K. W., Vogelstein, B., and Lengauer, C. Genetic instability and darwinian selection in tumours. Trends Cell Biol., *9:* M57–M60, 1999.
3. Jallepalli, P. V., and Lengauer, C. Chromosome segregation and cancer: cutting through the mystery. Nat. Rev. Cancer, *1:* 109–117, 2001.
4. Hahn, W. C., Counter, C. M., Lundberg, A. S., Beijersbergen, R. L., Brooks, M. W., and Weinberg, R. A. Creation of human tumour cells with defined genetic elements. Nature (Lond.), *400:* 464–468, 1999.
5. Hahn, W. C., and Weinberg, R. A. Modeling the molecular circuitry of cancer. Nat. Rev. Cancer, *2:* 331–341, 2002.
6. Hanahan, D., and Weinberg, R. A. The hallmarks of cancer. Cell, *100:* 57–70, 2000.
7. Li, R., Yerganian, G., Duesberg, P., Kraemer, A., Willer, A., Rausch, C., and Hehlmann, R. Aneuploidy correlated 100% with chemical transformation of Chinese hamster cells. Proc. Natl. Acad. Sci. USA, *94:* 14506–14511, 1997.
8. Lengauer, C., Kinzler, K. W., and Vogelstein, B. Genetic instability in colorectal cancers. Nature (Lond.), *386:* 623–627, 1997.
9. Auer, G. U., Heselmeyer, K. M., Steinbeck, R. G., Munck-Wikland, E., and Zetterberg, A. D. The relationship between aneuploidy and p53 overexpression during genesis of colorectal adenocarcinoma. Virchows Arch., *424:* 343–347, 1994.
10. Ried, T., Heselmeyer-Haddad, K., Blegen, H., Schrock, E., and Auer, G. Genomic changes defining the genesis, progression, and malignancy potential in solid human tumors: a phenotype/genotype correlation. Genes Chromosomes Cancer, *25:* 195–204, 1999.
11. Duesberg, P., Rasnick, D., Li, R., Winters, L., Rausch, C., and Hehlmann, R. How aneuploidy may cause cancer and genetic instability. Anticancer Res., *19:* 4887–4906, 1999.
12. Duesberg, P., Li, R., Rasnick, D., Rausch, C., Willer, A., Kraemer, A., Yerganian, G., and Hehlmann, R. Aneuploidy precedes and segregates with chemical carcinogenesis. Cancer Genet. Cytogenet., *119:* 83–93, 2000.
13. Simi, S., Musio, A., Vatteroni, L., Piras, A., and Rainaldi, G. Specific chromosomal aberrations correlated to transformation in Chinese hamster cells. Cancer Genet. Cytogenet., *62:* 81–87, 1992.
14. Rubin, H. Selected cells and selective microenvironment in neoplastic development. Cancer Res., *61:* 799–807, 2001.
15. Lengauer, C., Kinzler, K. W., and Vogelstein, B. Genetic instabilities in human cancers. Nature (Lond.), *396:* 643–649, 1998.
16. Eshleman, J. R., Casey, G., Kochera, M. E., Sedwick, W. D., Swinler, S. E., Veigl, M. L., Willson, J. K., Schwartz, S., and Markowitz, S. D. Chromosome number and structure both are markedly stable in RER colorectal cancers and are not destabilized by mutation of p53. Oncogene, *17:* 719–725, 1998.
17. Ghadimi, B. M., Sackett, D. L., Difilippantonio, M. J., Schrock, E., Neumann, T., Jauho, A., Auer, G., and Ried, T. Centrosome amplification and instability occurs exclusively in aneuploid, but not in diploid colorectal cancer cell lines, and correlates with numerical chromosomal aberrations. Genes Chromosomes Cancer, *27:* 183–190, 2000.
18. Peltomaki, P., and de la Chapelle, A. Mutations predisposing to hereditary nonpolyposis colorectal cancer. Adv. Cancer Res., *71:* 93–119, 1997.
19. Morales, C. P., Holt, S. E., Ouellette, M., Kaur, K. J., Yan, Y., Wilson, K. S., White, M. A., Wright, W. E., and Shay, J. W. Absence of cancer-associated changes in human fibroblasts immortalized with telomerase. Nat. Genet., *21:* 115–118, 1999.
20. Zucchi, I., Montagna, C., Susani, L., Montesano, R., Affer., M., Zanotti, S., Redolfi, E., Vezzoni, P., and Dulbecco, R. Genetic dissection of dome formation in a mammary cell line: identification of two genes with opposing action. Proc. Natl. Acad. Sci. USA, *96:* 13766–13770, 1999.
21. Mercatanti, A., Rainaldi, G., Mariani, L., and Citti, L. A method for prediction of accessible sites on a mRNA sequence for target selection of hammerhead ribozymes. J. Comput. Biol., *9:* 641–653, 2002.
22. Beigelman, L., McSwiggen, J. A., Draper, K. G., Gonzalez, C., Jensen, K., Karpeisky, A. M., Modak, A. S., Matulic-Adamic, J., DiRenzo, A. B., Haeberli, P., Sweedler, D., Tracz, D., Grimm, S., Wincott, F. E., Thackray, V. G., and Usman, N. Chemical modification of hammerhead ribozymes. Catalytic activity and nuclease resistance. J. Biol. Chem., *270:* 25702–25708, 1995.
23. Citti, L., Boldrini, L., Nevischi, S., Mariani, L., and Rainaldi, G. Quantitation of in vitro activity of synthetic trans-acting ribozymes using HPLC. Biotechniques, *23:* 898–903, 1997.
24. Elbashir, S. M., Martinez, J., Patkaniowska, A., Lendeckel, W., and Tuschl, T. Functional anatomy of siRNAs for mediating efficient RNAi in Drosophila melanogaster embryo lysate. EMBO J., *20:* 6877–6888, 2001.
25. Jablonski, S. A., Chan, G. K., Cooke, C. A., Earnshaw, W. C., and Yen, T. J. The hBUB1 and hBUBR1 kinases sequentially assemble onto kinetochores during prophase with hBUBR1 concentrating at the kinetochore plates in mitosis. Chromosoma, *107:* 386–396, 1998.
26. Musio, A., Rainaldi, G., and Sbrana, I. Spontaneous and aphidicolin-sensitive fragile site 3cen co-localize with (TTAGGG)n telomeric sequence in Chinese hamster cell. Cytogenet. Cell Genet., *75:* 159–163, 1996.
27. Schrock, E., du Manoir, S., Veldman, T., Schoell, B., Wienberg, J., Ferguson-Smith, M., Ning, Y., Ledbetter, D., Bar-Am, I., Soenksen, D., Garini, Y., and Ried, T. Multicolor spectral karyotyping of human chromosomes. Science (Wash. DC), *273:* 494–497, 1996.
28. Nowak, M. A., Komarova, N. L., Sengupta, A., Jalepalli, P. V., Shih, M., Vogelstein, B., and Lengauer, C. The role of chromosomal instability in tumor initiation. Proc. Natl. Acad. Sci. USA, *99:* 16226–16231, 2002.
29. Koshland, D., and Strunnikov, A. Mitotic chromosome condensation. Annu. Rev. Cell Dev. Biol., *12:* 305–333, 1996.
30. Cahill, D. P., Lengauer, C., Yu, J., Riggins, G. J., Willson, J. K., Markowitz, S. D., Kinzler, K. W., and Vogelstein, B. Mutations of mitotic checkpoint genes in human cancers. Nature (Lond.), *392:* 300–303, 1998.
31. Earnshaw, W. C., Martins, L. M., and Kaufmann, S. H. Mammalian caspases: structure, activation, substrates, and functions during apoptosis. Annu. Rev. Biochem., *68:* 383–424, 1999.
32. Bond, J. A., Haughton, M. F., Rowson, J. M., Smith, P. J., Gire, V., Wynford-Thomas, D., and Wyllie, F. S. Control of replicative life span in human cells: barriers to clonal expansion intermediate between M1 senescence and M2 crisis. Mol. Cell. Biol., *19:* 3103–3114, 1999.
33. Biedermann, K. A., and Landolph, J. R. Induction of anchorage independence in human diploid foreskin fibroblasts by carcinogenic metal salts. Cancer Res., *47:* 3815–3823, 1987.
34. Kolman, A., Kotova, N., and Grawe, J. Aphidicolin induces 6-thioguanine resistant mutants in human diploid fibroblasts. Mutat. Res., *499:* 227–233, 2002.
35. Shay, J. W., and Wright, W. E. Hayflick, his limit, and cellular aging. Nat. Rev. Mol. Cell Biol., *1:* 72–76, 2000.
36. Mathon, N. F., and Lloyd, A. C. Cell senescence and cancer. Nat. Rev. Cancer, *1:* 203–213, 2001.
37. DePinho, R. A. The age of cancer. Nature (Lond.), *408:* 248–254, 2000.
38. Bodnar, A. G., Ouellette, M., Frolkis, M., Holt, S. E., Chiu, C. P., Morin, G. B., Harley, C. B., Shay, J. W., Lichtsteiner, S., and Wright, W. E. Extension of life-span by introduction of telomerase into normal human cells. Science (Wash. DC), *279:* 349–352, 1998.
39. Jiang, X. R., Jimenez, G., Chang, E., Frolkis, M., Kusler, B., Sage, M., Beeche, M., Bodnar, A. G., Wahl, G. M., Tlsty, T. D., and Chiu, C. P. Telomerase expression in human somatic cells does not induce changes associated with a transformed phenotype. Nat. Genet., *21:* 111–114, 1999.
40. Heim, S., and Mitelman, F. (eds.). Cancer Cytogenetics. New York: Wiley-Liss, Inc., 1987.
41. Dobles, M., Liberal, V., Scott, M. L., Benezra, R., and Sorger, P. K. Chromosome missegregation and apoptosis in mice lacking the mitotic checkpoint protein Mad2. Cell, *101:* 635–645, 2000.
42. Michel, L. S., Liberal, V., Chatterjee, A., Kirchwegger, R., Pasche, B., Gerald, W., Dobles, M., Sorger, P. K., Murty, V. V., and Benezra, R. MAD2 haplo-insufficiency causes premature anaphase and chromosome instability in mammalian cells. Nature (Lond.), *409:* 355–359, 2001.